*Korean J. Chem. Eng.*, 33(2), 616-622 (2016)
DOI: 10.1007/s11814-015-0149-0

pISSN: 0256-1115
eISSN: 1975-7220

# Preparation of nanoporous activated carbon and its application as nano adsorbent for $CO_2$ storage

**Ali Morad Rashidi*,†, Davood Kazemi*, Nosrat Izadi*, Mahnaz Pourkhalil*, Abbas Jorsaraei*, Enseyeh Ganji**, and Roghayeh Lotfi***

*Nanotechnology Research Center, Research Institute of Petroleum Industry, Tehran, Iran
**Gas Division, Research Institute of Petroleum Industry, Tehran, Iran
(*Received 17 December 2014 • accepted 10 July 2015*)

**Abstract**−Nanoporous activated carbons, as adsorbent for $CO_2$ storage, were prepared from walnut shells via two chemical processes including phosphoric acid treatment and KOH activation at high temperature. Specific surface area and porosities were controlled by KOH concentration and activation temperature. The obtained adsorbents were characterized by $N_2$ adsorption at 77.3 K. Their carbon dioxide adsorption capacities were measured at different pressures at 290 K by using volumetric adsorption equipment. The KOH-treated nanoporous carbons typically led to the production of high specific surface areas and high micropore volumes and showed better performance for $CO_2$ adsorptions. The maximum experimental value for adsorption capacity happened when pressure increased from 5 to 10 bar (1.861-2.873 $mmol \cdot g^{-1}$). It was found that in order to improve the highest capacity of $CO_2$ adsorption for KOH-modified carbon (9.830-18.208 $mmol \cdot g^{-1}$), a KOH: C weight ratio of 3.5 and activation temperature of 973 K were more suitable for pore development and micro-mesopore volume enhancement.

Keywords: Nanoporous Activated Carbon, KOH Treatment, $CO_2$ Storage, Adsorption

## INTRODUCTION

Combustion of fossil fuels is one of the major sources of greenhouse gases (e.g. $CO_2$) upsurge. It is necessary to develop technologies that minimize the propagation of greenhouse gases while utilizing the fossil fuels. Commercial $CO_2$ capture technologies such as cryogenic distillation and membrane filtration are very expensive and energy intensive [1]. The lessening of carbon dioxide emissions from flue gases can be achieved using post-combustion capture technologies such as adsorption. Pressure swing adsorption (PSA) is an improved potential technology for $CO_2$ capture from high pressure gas streams [1,2]. It is based on the adsorption of $CO_2$ gas over porous materials at high pressures. Swinging to low pressures desorbs the gas and regenerates the sorbent. PSA technology has attracted much attention for low energy requirements and low capital investment costs [1]. Due to their highly developed porous structure porous materials, such as molecular sieves, zeolites and activated carbons are apt for $CO_2$ capture [3-5]. Low cost, high $CO_2$ adsorption capacity, ease of regeneration and lower sensitivity to the moisture are some of the advantages of activated carbons in due course. In particular, micro and meso porosities of the activated carbons with large surface areas make them pertinent to a wide range of industrial and technological processes [6]. Based in the size of pores, they are micropores (diameters <2 nm), mesopores (diameters 2-50 nm) or macropores (diameters >50 nm). The performance of activated carbons is closely related to their adsorption characteristics such as mean pore size, pore size distribution, specific pore volume and density [7]. In general raw materials such as bituminous coal, pistachio shell, coconut shell, walnut shell, coir pith, cassava peal, fir wood, oil-palm shell, sugarcane bagasse, babassu and corncob are treated to form charcoal; physical or chemical activation of the charcoal results in activated carbons. In the carbonization process, the starting material is pyrolyzed below 800 °C in an inert atmosphere so that the volatile matter is removed and the rudimentary carbonaceous structure is left behind. Activating agents, such as air, steam or carbon dioxide, initiate the process. Different raw materials produce activated carbons with different qualities [8]. Nitrogen-containing functional groups increase the capacity of the physical $CO_2$ adsorption of activated carbons. Modification of activated carbon has attracted considerable attention in order to enhance the effectiveness of carbon dioxide capture [9-24].

In this work, high specific surface area nanoporous carbons containing micro-meso pore volumes were prepared by phosphoric acid and KOH treatment. The nanoporous carbons were then carbonized at 700-900 °C to control the pore size and increase $CO_2$ capture capacity.

## EXPERIMENTAL

### 1. Initial Activated Carbon and Textural Modification Technique

To produce activated carbon, walnut shells were used as the starting material in all experiments. Two steps of activation processes including phosphoric acid and KOH treatment were then followed. In comparison with other resources, walnut shells were used in this work for of their low-price, abundance, high strength and high cellulose content in Iran.

†To whom correspondence should be addressed.
E-mail: rashidiam@ripi.ir

During phosphoric acid activation, walnut shells were soaked with phosphoric acid for 12 h in an oven at 150 °C. Then the resulting material was cooled to room temperature. Treated carbon was then washed with a mixture of hot water and hydrochloric acid and neutralized with water. In the second step, to prepare the predetermined ratios, weighted amounts of the precursor (H-AC) and KOH were mixed (R=KOH/C). After drying at 150 °C for 2 h, the sample was activated by putting the mixture on a ceramic boat in a tubular electric furnace under a nitrogen flow rate of 200 ml $min^{-1}$. The thermal treatment consisted of heating from ambient temperature to the final temperature with a heating rate of 5 °C $min^{-1}$, followed by a 1 h isothermal period and the final cooling down to room temperature. By repeated rinsing with hot distilled water, the sample was neutralized. To remove the residual water, the product was dried in air for 24 h at 120 °C. The abbreviations for the six different samples are defined in Table 1. In this table, H-AC is a walnut-based carbon manufactured by phosphoric acid (85% solution) activation process; while KH-AC is a post KOH-treated activated carbon with nanoporous structure. The numbers 72, 82, etc., represent the first digits of the activation temperature and reagent to base ratio; for instance, 72 stands for a temperature of 700 °C and reagent to base ratio of 2.5.

**Table 1. Activation temperature, reagent to base for walnut shell**

| Sample | Activation temperature (°C) | Activating reagent | Reagent to base |
|---|---|---|---|
| H-AC | 550 | $H_3PO_4$ | 1.25 |
| KH-AC-72 | 700 | KOH | 2.50 |
| KH-AC-82 | 800 | KOH | 2.50 |
| KH-AC-92 | 900 | KOH | 2.50 |
| KH-AC-73 | 700 | KOH | 3.50 |
| KH-AC-83 | 800 | KOH | 3.50 |
| KH-AC-93 | 900 | KOH | 3.50 |

**2. Accelerated Surface Area and Porosimetry Analysis (ASAP)**

For all samples, accelerated surface area and porosimetry analysis was carried out with sub-critical nitrogen at 77.3 K on a model 2010 Micromeritics American Instrument, which was calibrated by using the surface area of the $Al_2O_3$ reference material. Prior to ASAP measurement, samples were heated at 30 °C and 200 °C for 30 and 180 min (with heating rate of 10 °C $min^{-1}$) under $N_2$ gas flow of 40 mL $min^{-1}$ to remove any adsorbed species. Then the samples were cooled to room temperature under $N_2$ flow.

Specific surface areas were determined from sub-critical nitrogen isotherms by using Brunauer-Emmett-Teller (BET) theory in the $P/P_0$ range of 0.06-0.2. The total pore volume was determined at $P/P_0$=0.995. The t-plot method was applied to calculate the micropore volume. Also $S_{BET}$ (specific surface area) was determined from BET equation at $P/P_0$=0.05-0.1; $V_{micro}$ (micropore volume) was calculated from Dubinin-Radushkevich equation; $V_{meso}$ (mesopore volume) was determined from BJH equations; $V_{total}$ (total pore volume) was calculated by $V_{ads}$ ($P/P_0$=0.995)×0.001547 and D (average pore diameter) is calculated by 4V/A from BET equation.

**3. Apparatus and $CO_2$ Adsorption Capacity Experiments**

$CO_2$ adsorption experiments were carried out in a stainless steel

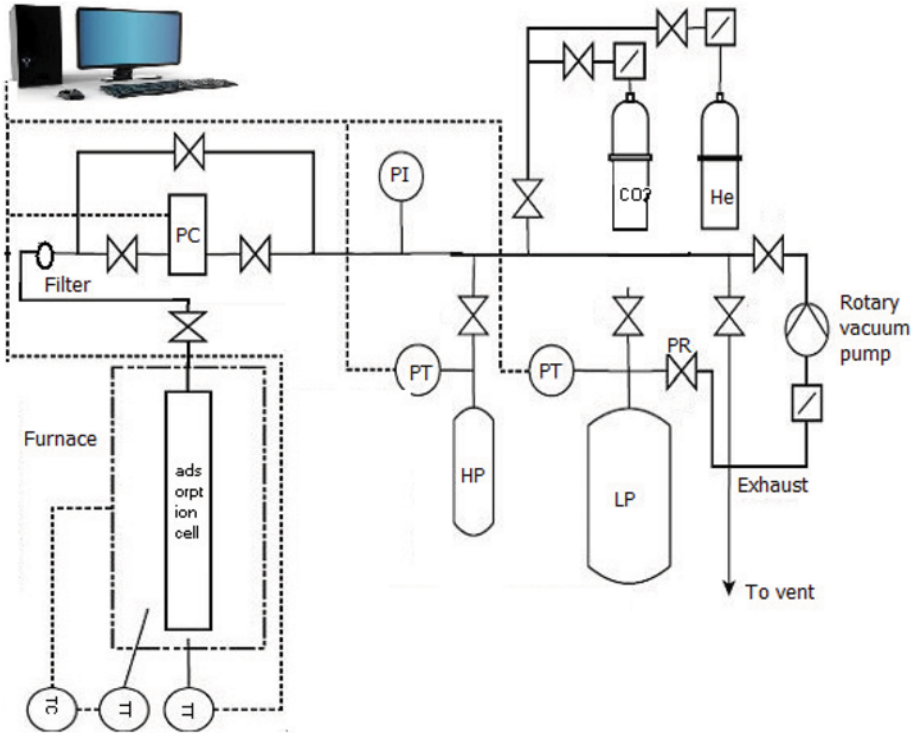


**Fig. 1. Schematic adsorption test set-up.**

PR. Pressure relief valve
PC. Pressure controller
PI. Pressure indicator
PT. Pressure transmitter
TT. Temperature transmitter
TC. Temperature controlller

adsorption system (Fig. 1). The adsorption column was a small stainless steel basket packed with 40 to 60 mesh carbon samples. The vacuum before adsorption was at the range of $10^{-3}$ to $10^{-4}$ bar. Before the experiments, the carbon samples were dried in vacuum at 200 °C for 4 h (degassing process). Helium was used to measure the volume of the void space in the adsorption cell. The purity of helium and carbon dioxide was higher than 99.9999%. Up to 30 bar, pressure was measured at different intervals with a sensitivity of 0.01%. The temperature was kept constant at 17 °C. The main goal this study was to determine the adsorption capacity of the adsorbed $CO_2$ at different equilibrium pressures. In general the amount of the adsorbed material in the equilibrium condition was measured by volumetric and gravimetric methods. In this work, the volumetric method was used. In this method, the pressure drop was measured in a closed system before and after adsorption. The amount of adsorbed gas was calculated by a suitable equation of state in a specified pressure and volume. Before $CO_2$ injection, the void space of the adsorption cell was determined for the measurement of the adsorbed gas in the micropores. The void is consisted of macropores volume as well as the space between the activated carbon particles. After helium injection at a specified pressure and temperature, the void was calculated by a suitable PVT relationship. The $CO_2$ injection was after void calculation. Because of the adsorption, continuously the cell pressure reduced until the equilibrium condition was reached. The amount of the adsorbed gas was measured through final pressure and the characteristics of the adsorption cell. The model was designed with the aid of MATLAB toolboxes, which gave the best response for the correlation of carbon dioxide uptake of activated carbon sample.

## RESULTS AND DISCUSSION

### 1. Sub-critical Nitrogen Adsorption

The nitrogen adsorption/desorption isotherms of all samples at 77.3 K are represented in Fig. 2. According to IUPAC classification, Type I isotherm is concave on $P/P_0$ axis and $n^a$ approaches a limiting value as $P/P_0 \rightarrow 1$. Type I isotherms are known for microporous solids with pore size of <2 nm. On the other hand, hysteresis loop is representative of type IV isotherms, which is accompanied by capillary condensation in mesopores and limiting uptake over a range of high $P/P_0$. The initial part of type IV isotherm is characteristic of monolayer-multilayer adsorption, since it follows the same path as the corresponding part of the Type II isotherm obtained with the given adsorption on the same surface area of the adsorbent in a non-porous form. From Fig. 2, adsorption/desorption isotherms of H-AC, KH-AC-72, KH-AC-82 and KH-AC-83 show behavior similar to Type I isotherm, which is mainly related to the microporous materials. On the other hand, the adsorption/desorption isotherms for KH-AC-93 and KH-AC-73 show type IV behavior with both micro and meso porosities. The KH-AC-92 also showed type IV isotherm with their characteristic hysteresis loop at relative pressures higher than 0.01 and revealed only mesoporosity. For H-AC, KH-AC-72, KH-AC-82 and KH-AC-83 due to multidirectional interactions between the pore walls and the adsorbent, the adsorption happened at very low relative pressure regions ($P/P_0<0.3$). because of the multidirectional interactions between the pore walls and the adsorbents in KH-AC-93 and KH-AC-73, in the beginning the adsorption took place at very low relative pressure regions ($P/P_0<0.3$); then the hysteresis loop was associated with the secondary process of capillary condensation, which resulted in complete filling of the mesopores at $0.4<P/P_0<1$. For KH-AC-92 with no micropores, the adsorption took place at high relative pressure regions ($P/P_0<1$) with the capillary condensation, which only resulted in the filling of the mesopores. Treatment of the H-AC carbon with KOH caused an increase in the volume of adsorbed $N_2$ by the car-

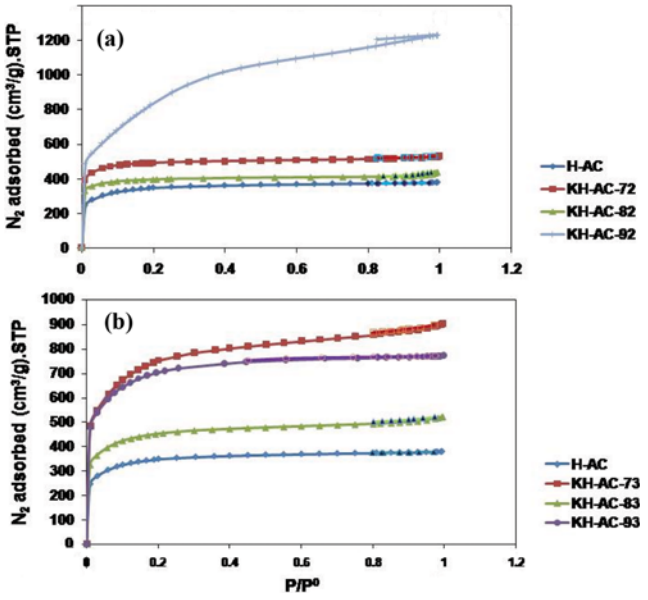


**Fig. 2. The $N_2$ adsorption/desorption isotherms for treated nanoporous carbons at different temperatures (a): KOH/C=2.5, (b): KOH/C=3.5.**

**Table 2. Textural parameters of the modified activated carbons**

| Samples | $S_{BET}$ ($m^2$/g) | $V_{micro}$ ($cm^3$/g) | $V_{meso}$ ($cm^3$/g) | $V_{total}$ ($cm^3$/g) | $F_{micro}$ (%) | $F_{meso}$ (%) | D (nm) |
|---|---|---|---|---|---|---|---|
| H-AC | 1260.98 | 0.32 | 0.26 | 0.58 | 55.17 | 44.83 | 1.86 |
| KH-AC-72 | 1527.19 | 0.62 | 0.20 | 0.82 | 75.61 | 24.39 | 2.17 |
| KH-AC-82 | 1538.44 | 0.51 | 0.16 | 0.67 | 76.11 | 23.89 | 2.00 |
| KH-AC-92 | 3143.47 | 0.32 | 1.67 | 1.90 | 4.73 | 104.73 | 2.46 |
| KH-AC-73 | 2642.56 | 0.46 | 0.93 | 1.39 | 33.09 | 66.91 | 2.11 |
| KH-AC-83 | 1689.60 | 0.43 | 0.37 | 0.80 | 53.75 | 46.25 | 1.93 |
| KH-AC-93 | 2429.57 | 0.53 | 0.66 | 1.19 | 44.53 | 55.47 | 1.96 |

bon samples. On the other hand, for KOH treated active carbons, the knees of the isotherms at $P/P_0$=0.01, were sharper than those of the isotherms of H-AC samples. In all KOH treated active carbons except KH-AC-92, the micropore structure developed significantly in comparison with the H-AC samples. Table 2 contains the textural parameters calculated from $N_2$ adsorption isotherms at 77.3 K.

It was observed that for samples with the ratio of KOH/H-AC= 2.5, with increasing the carbonization temperature the specific surface area increased significantly, but the micropore structure decreased abruptly such that for KH-AC-92 it reaches −0.09 (Table 2). Also, as shown in Table 2, for samples with the ratio of KOH/H-AC= 3.5, with increasing carbonization temperature, the specific surface area and micropore volume decreased and then increased in KH-AC-93 sample. At constant temperature, increasing the KOH/C weight ratio decreased the mean pore diameter of the porous carbons. Also, except for KH-AC-9 an increase in the specific surface area and mesopore volume and a significant decrease in micropore volume were observed. In fact, it seems that increasing the KOH/C weight ratio would increase the amount of penetration of metallic potassium into the carbon matrix. Consequently, the carbon matrix would be more and more enlarged and the mesoporosity would be increased. The activation process with KOH has been described by Otowa et al. [25]. They explained that below 700 °C, the main products are $H_2$, $H_2O$, CO, $CO_2$, $K_2O$ and $K_2CO_3$ according to the following reactions:

$$2KOH \rightarrow K_2O + H_2O$$
$$C + H_2O \rightarrow CO + H_2$$
$$CO + H_2O \rightarrow CO_2 + H_2$$
$$CO_2 + K_2O \rightarrow K_2CO_3$$

Above 700 °C, an important activation mechanism including the formation of metallic potassium occurs according to the following reaction:

$$K_2O + H_2 \rightarrow 2K + H_2O$$
$$K_2O + C \rightarrow 2K + CO$$

Moreover, the rate of heating, final temperature, soaking time and the weight ratio are important parameters that determine the quality and the yield of the carbonized product. In this work, the activation process by phosphoric acid generated a surface area of 1,260 $m^2/g$ and micropore volume of 0.32 $cm^3/g$. Additional KOH activation permits an increase in the surface area and micropore volume by a factor of 1.68 and 1.33, respectively. At 700 °C and 800 °C, by increasing the KOH/C weight ratio, an increase in the surface area by a factor of 1.73 and 1.26 and a decrease in micropore volume by a factor of 0.26 and 0.16 were observed, respectively. While in 900 °C, an increase of 100% in micropore volume and a decrease of 23% in specific surface area were observed. Probably at KOH/C=2, heat treatment up to 900 °C had led to the hardening of carbon structure due to partial alignment of graphitic planes and consequently the micropore volume was reduced. The pore size distribution of activated carbon in cumulative pore volume and differential pore volume are presented in Figs. 3 and 4.

TEM image of nanoporous carbon is shown in Fig. 5. As it can be seen, the carbon layers shift to the graphene sheet as indicated

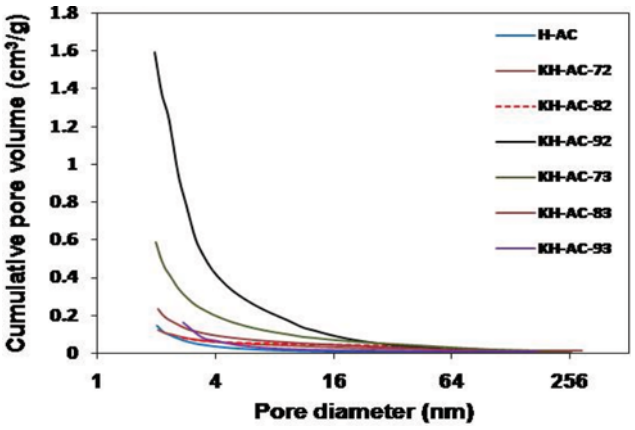


**Fig. 3. Pore size distribution of prepared nanoporous carbons ($N_2$/77.3 K)-cumulative pore volume.**

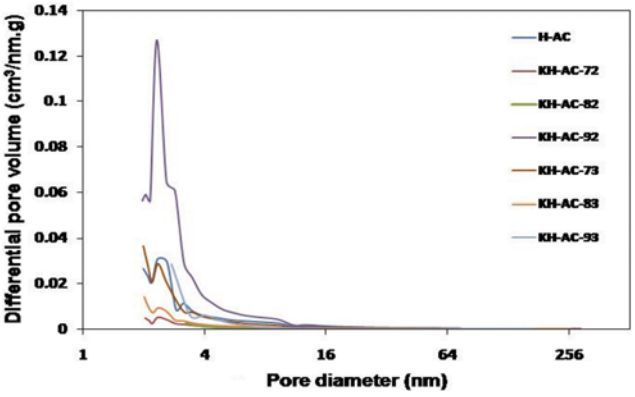


**Fig. 4. Pore size distribution of prepared nanoporous carbons ($N_2$/77.3 K)-differential pore volume.**

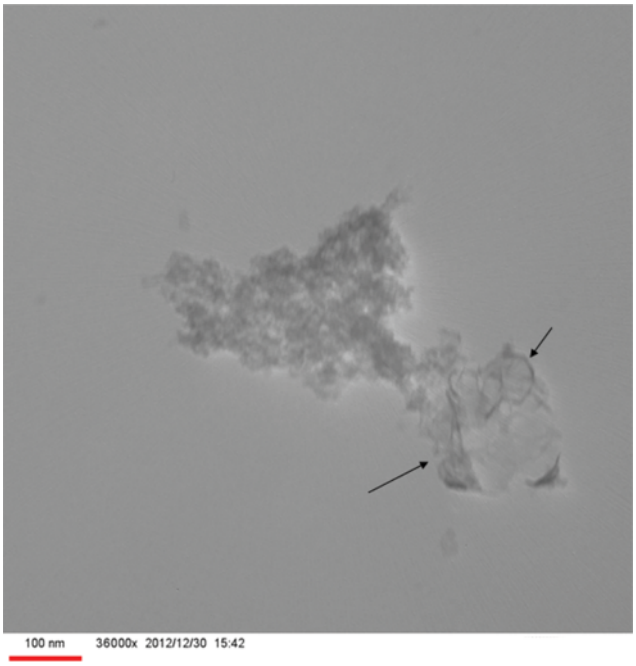


**Fig. 5. TEM image of nanoporous carbon at KOH/C=3.5, and 973 K.**

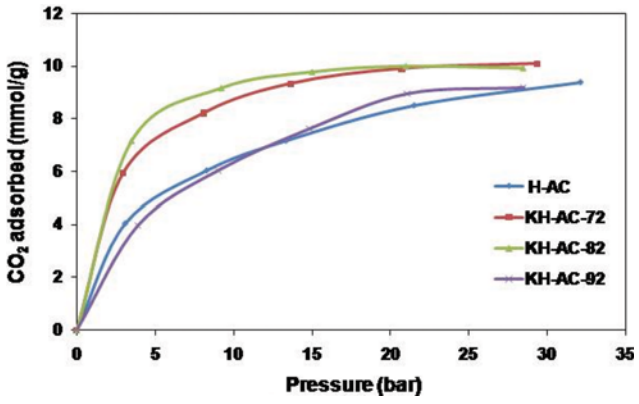


Fig. 6. $CO_2$ adsorption isotherms of the prepared nanoporous carbons treated with phosphoric acid and KOH (KOH:C=2.5) at T=290 K and different pressure (influence of activation temperature).

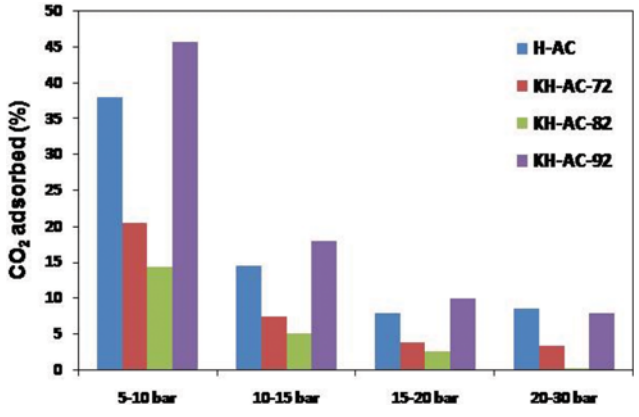


Fig. 7. Comparison of $CO_2$ adsorption content of the prepared nanoporous carbons treated with phosphoric acid and KOH (KOH:C=2.5) at T=290 K and different pressure. Increasing rate of $CO_2$ adsorption amount depends on reaction pressure.

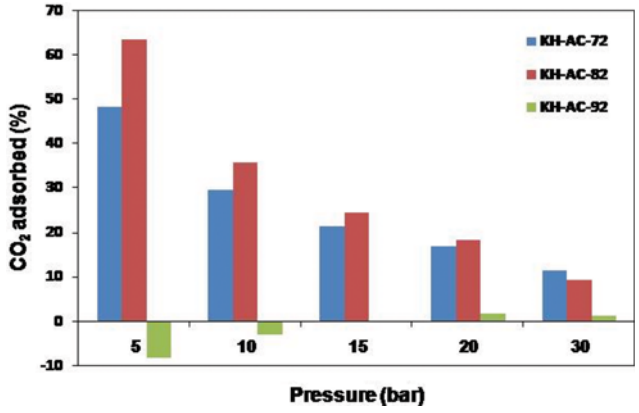


Fig. 8. Comparison of the $CO_2$ adsorption content of the prepared nanoporous carbons treated with KOH (KOH:C=2.5) versus H-AC carbon at T=290 K and different pressures. Increasing rate of $CO_2$ adsorption amount depends on reaction pressure.

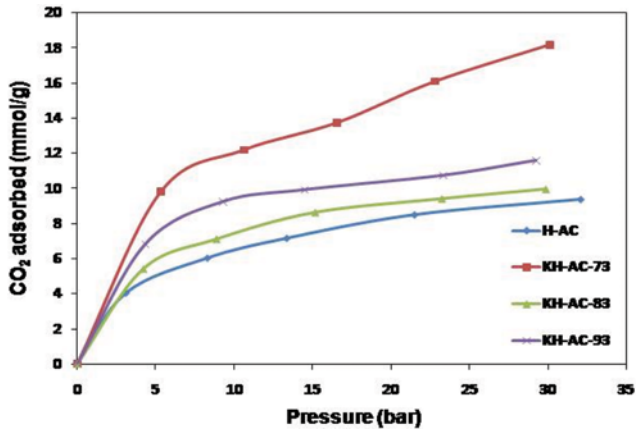


Fig. 9. $CO_2$ adsorption isotherms of the prepared nanoporous carbons treated with phosphoric acid and KOH (KOH:C=3.5) at T=290 K and different pressure (influence of activation temperature).

by the arrow. This structure causes an increase in the surface area and the pore volume of the nano adsorbent.

**2. Evaluation of $CO_2$ Isotherms on Nanoporous Carbons**

2-1. $CO_2$ Isotherms on KOH-modified Activated Carbon (KOH:C=2.5) at Different Temperatures

The sorption isotherms and adsorption capacity of $CO_2$ at 290 K are shown in Figs. 6 and 7. Note that the concept of absolute adsorption amount, which is the total number of adsorptive molecules that are located within the adsorbate volume, has been used. As shown in Fig. 6, except for KH-AC-92, the $CO_2$ adsorption performance of KOH-treated nanoporous carbons was better than the H-AC ones. When pressure increased from 5 to 10 bar, the highest $CO_2$ adsorption rate was observed for all samples, (Fig. 7). The adsorbed weights ($CO_2$) of all carbonaceous species at moderate pressure range (up to 20 bar) are in the following order: KH-AC-82>KH-AC-72>H-AC>KH-AC-92. At 30 bar, the KH-AC-72 has a higher $CO_2$ capture in comparison with the KH-AC-82 (Fig. 8). At 5 to 20 bar (Fig. 5), KH-AC-82 sample with a micropore volume of 0.51 $cm^3/g$ has the highest $CO_2$ capture. The KOH activation process of KH-AC-82 in comparison with the H-AC samples, led to increased $CO_2$ capture by a factor of 1.64, 1.36, 1.24 and 1.18 at pressures of 5, 10, 15 and 20 bar, respectively. But at 30 bar, the KH-AC-72 with a micropore volume of 0.61 $cm^3/g$ had the highest adsorbed $CO_2$ concentration (11.34%). This trend is in agreement with the results of Py et al. [26]. According to their study, larger micropore volume requires higher pressure to be efficiently used for storage purpose. At 900 °C, the micropore volume decreased suddenly and the total pore volume including the mesopore volume increased;, as a result larger pore diameter was created. In this case for $CO_2$ adsorption showed no advantage over H-AC carbon material.

2-2. $CO_2$ Isotherms on KOH-modified Activated Carbon (KOH:C=3.5) at Different Temperatures

$CO_2$ adsorption capacity of nanoporous carbons was measured using $CO_2$ adsorption isotherms at 290 K, as shown in Figs. 8 and 9. From data presented in Fig. 9, all samples have better performance in $CO_2$ capture than H-AC carbon. In all samples, the high-

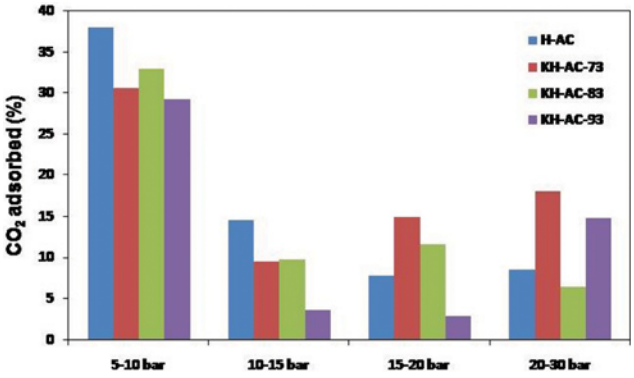


**Fig. 10. Comparison of $CO_2$ adsorption content of the prepared nanoporous carbons treated with phosphoric acid and KOH (KOH:C=3.5) at T=290 K and different pressure.**

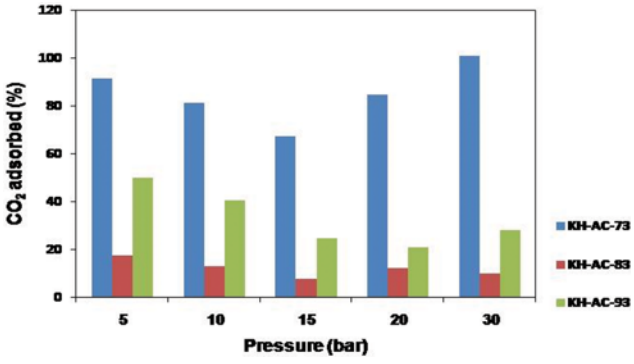


**Fig. 11. Comparison of $CO_2$ adsorption content of the prepared nanoporous carbons treated with KOH (KOH:C=3.5) related to H-AC carbon at T=290 K and different pressure.**

est $CO_2$ adsorption rate occurs when pressure increases from 5 to 10 bar (Fig. 10). The adsorbed $CO_2$ weights of all carbon species at moderate relative pressure range (up to 30 bar) are in the following order: KH-AC-73>KH-AC-93>KH-AC-83>H-AC. The highest $CO_2$ capture occurs at all pressures for KH-AC-73 sample with a micropore volume of 0.46, mesopore volume of 0.93 and pore diameter of 2.1 nm (Fig. 11). For this sample, the activation process by KOH produces an adsorbed $CO_2$ concentration increase by a factor of 1.91, 1.81, 1.73, 1.85 and 2.04 at pressures of 5, 10, 15, 20 and 30 bar, respectively, when compared with H-AC sample.

2-3. Comparison of $CO_2$ Isotherms

At 700 °C, by increasing the KOH:C weight ratio, the adsorbed $CO_2$ at 290 K increased by a factor of 1.29, 1.39, 1.42, 1.58 and 1.80 at pressures of 5, 10, 15, 20 and 30 bar, respectively (Fig. 12). At this temperature, by increasing the KOH:C weight ratio, the specific surface area increased but the micropore volume and pore diameter decrease. From Fig. 2, the $N_2$ adsorption/desorption isotherms of KH-AC-72 show Type I behavior, which is mainly characteristic of microporous materials. However, the $N_2$ adsorption/desorption isotherms for KH-AC-73 show Type IV with both micro-meso porosity. In fact, the samples with characteristic of mainly micro-mesoporous materials have better performance for $CO_2$ capture at 290 K. At 800 °C, we observe a decrease in $CO_2$ concentration by

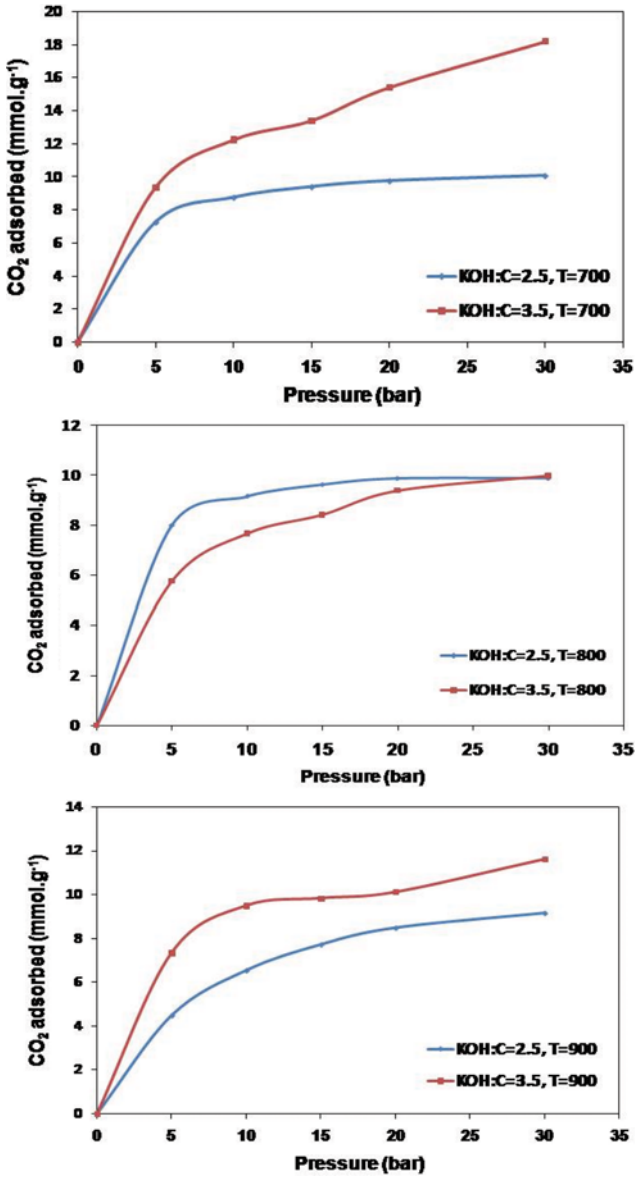


**Fig. 12. $CO_2$ adsorption isotherms of the prepared nanoporous carbons treated with KOH at T=290 K and different pressure (influence of weight ratio).**

increasing the KOH:C weight ratio. At 900 °C, an increase in $CO_2$ capture occurs by increasing the KOH:C weight ratio. The samples of KH-AC-92 and KH-AC-93 also show Type IV isotherm with hysteresis loop at relative pressures above 0.01. But KH-AC-92 exhibit only mesoporosity and no microporosity; therefore, it is not suitable for $CO_2$ capture. Also Fig. 13 shows that KH-AC-73 has a maximum $CO_2$ adsorption of 9.38, 12.25, 13.42, 15.42 and 18.20 mmol $g^{-1}$ at pressures of 5, 10, 15, 20 and 30 bar, respectively. These results can be compared with Gil et al. [17], which reported $CO_2$ adsorption of 7.36 to 11.22 mmol $g^{-1}$ at pressure of 10 bar for different KOH-activated carbons. They also measured the $CO_2$ adsorption of a commercial sample (Maxsorb) which was 13.63 mmol $g^{-1}$ at 10 bar. According to Park's study [27], the pore distribution is a key factor in developing a carbon material with higher $CO_2$

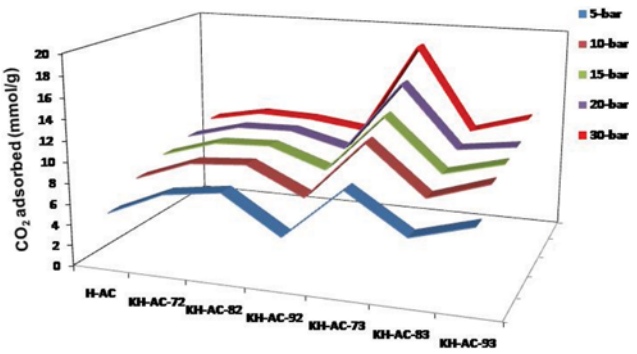


**Fig. 13. Comparison of $CO_2$ adsorption contents of the prepared nanoporous carbons treated with phosphoric acid and KOH at T=290 K and different pressure.**

adsorption capacity. Park explained that more $CO_2$ adsorption is due to condensation in the space available within the mesopores. As pressure increases, the physical properties of the adsorbent, such as specific surface area and micropore volume, become more important for $CO_2$ adsorption. This is because high micropore volume means more adsorption sites available and large pore volume means more space available for $CO_2$ capture. This trend is in accordance with what is observed in this study for KH-AC-73. This sample with a pore diameter of 2.1 nm is composed of 33% micropore volume and 67% mesopore volume and has the maximum $CO_2$ capture. According to Romono et al. [28] by increasing the KOH:C weight ratio, penetration escalation of metallic potassium into the carbon matrix, results in more porosity. Thus $CO_2$ adsorption at 290 K predominantly depends on the KOH:C weight ratio and the activation temperature is not a key factor.

## CONCLUSION

The results obtained reflect the synthesis of heat-treated activated carbons as nano adsorbent for $CO_2$ capture, prepared from walnut shells via two chemical stages, phosphoric acid treatment followed by KOH activation at different temperatures and different weight ratios. The KOH-treated nanoporous carbons generated both high specific surface area and high micro-meso pore volume and showed better performance for $CO_2$ adsorption. In all samples, the maximum experimental value for adsorption capacity rate happened when pressure was increased from 5 to 10 bar (1.861-2.873 $mmol \cdot g^{-1}$). The KOH:C weight ratio of 3.5 and activation temperature of 973 K were more suitable for pore development (2.1 nm) and micro-mesopore volume (0.46-0.93 $cm^3 \cdot g^{-1}$) in order to improve the highest capacity for $CO_2$ adsorption in nanoporous KOH-modified carbons (9.830-18.208 $mmol \cdot g^{-1}$). The high capture capacity of $CO_2$ by physical adsorption into narrow pore channels could be manipulated by control of pores.

## REFERENCES

1. R. Siriwardance, M. Shen, E. Fisher, J. Poston and D. H. Smith, U.S Department of energy, National energy technology laboratory, 3610 Collins Ferry Road, Morgantown, WV 26507-0880.
2. B. K. Na, K. K. Koo, H. M. Eum, H. Lee and H. K. Song, *Korean J. Chem. Eng.*, **18**, 220 (2001).
3. K. S. Hwang, S. Y. Gong and W. K. Lee, *Korean J. Chem. Eng.*, **8**, 148 (1991).
4. X. Xu, C. Song, J. M. Andresen, B. G. Miller and A. W. Scaronl, *Energy Fuels*, **16**, 1463 (2002).
5. R. V. Siriwardance, M.-S. Shen and E. P. Fisher, *Energy Fuels*, **19**, 1153 (2005).
6. R. C.Bansal, J. Dannet and F. Stoectdi, *Activated carbon*, Marcel Dekker (1998).
7. B. Buczek, A. Światkowski, S. Zietek and B. J. Trznadel, *Fuel*, **79**, 1247 (2000).
8. Wan Mohd Ashri Wan Daud, Wan Shabuddin and Mohd Zaki Sulaiman, *Carbon*, **38**, 1925 (2000).
9. A. Arenillas, K. M. Smith, T. C. Drage and C. E. Snape, *Fuel*, **84**, 2204 (2005).
10. T. C. Drage, A. Arenillas, K. M. Smith, C. Pevida, S. Piippo and C. E. Snape, *Fuel*, **86**, 22 (2007).
11. M. L. Gray, Y. Soong, K. J. Champagne, J. Baltrus, R. W. Stevens Jr., P. Toochinda and S. S. S. Chuang, *Sep. Purif. Technol.*, **35**, 31 (2004).
12. H. Y. Huang, R. T. Yang, D. Chinn and C. L. Munson, *Ind. Eng. Chem. Res.*, **42**, 2427 (2003).
13. M. M. Maroto-Valter, Z. Tang and Y. Zhang, *Fuel Process. Technol.*, **86**, 1487 (2005).
14. J. Przepiorski, M. Skrodzewicz and A. W. Morawsid, *Appl. Surf. Sci.*, **225**, 335 (2004).
15. M. G. Plaza, C. Pevida, A. Arenillas, F. Rubiera and J. J. Pis, *Fuel*, **86**, 2204 (2007).
16. M. G. Plaza, C. Pevida, B. Arias, J. Fermoso, A. Arenillas, F. Rubiera, J. J. Pis and J. Them, *Anal. Cal.*, **92**, 601 (2008).
17. R. R. Gil, B. Ruiz, M. S. Lozano and E. Fuente, *J. Anal. Appl. Pyrol.*, **110**, 194 (2014).
18. M. Balsamo, T. Budinova, A. Erto, A. Lancia, B. Petrova, N. Petrov and B. Tsyntsarski, *Sep. Purif. Technol.*, **116**, 214 (2013).
19. C. Robertson and R. Mokaya, *Micropor. Mesopor. Mater.*, **179**, 151 (2013).
20. B. Guo, L. Chang and K. Xie, *J. Nat. Gas Chem.*, **15**, 223 (2006).
21. S. Himeno, T. Komatsu and S. Fujita, *J. Chem. Eng. Data*, **50**, 369 (2005).
22. M. Sevilla and A. B. Fuertes, *J. Colloid Interface Sci.*, **366**, 147 (2012).
23. B. J. Kim, K. S. Cho and S. J. Park, *J. Colloid Interface Sci.*, **342**, 575 (2010).
24. L. Y. Meng and S. J. Park, *Mater. Chem. Phys.*, **137**, 91 (2012).
25. T. Otowa, R. Tanibata and M. Itoh *Gas Sep. Purif.*, **7**, 241 (1993).
26. X. Py, V. Goetz and G. Plantard, *Chem. Eng. Process.*, **47**, 308 (2008).
27. L.-Y. Meng and S.-J. Park, *Bull. Korean Chem. Soc.*, **33**, 3749 (2012).
28. J. Romanos, M. Beckner, T. Rash, L. Firlej, B. Kuchta, P. Yu, G. Suppes, C. Wexler and P. Pfeifer, *Nanotechnology*, **23**, 015401 (2012).